This article was downloaded by:
On: *25 January 2011*
Access details: *Access Details: Free Access*
Publisher *Taylor & Francis*
Informa Ltd Registered in England and Wales Registered Number: 1072954 Registered office: Mortimer House, 37-41 Mortimer Street, London W1T 3JH, UK

Separation Science and Technology
Publication details, including instructions for authors and subscription information:
http://www.informaworld.com/smpp/title~content=t713708471

Modeling Concentration Polarization Phenomena for Shell-Side Flow in Ultrafiltration Process

Sergei P. Agashichev[a]
[a] DEPARTMENT OF CHEMICAL ENGINEERING, MENDELEJEV UNIVERSITY, MOSCOW A-47, RUSSIA

Online publication date: 29 January 1999

To cite this Article Agashichev, Sergei P.(1999) 'Modeling Concentration Polarization Phenomena for Shell-Side Flow in Ultrafiltration Process', Separation Science and Technology, 34: 2, 243 — 261
To link to this Article: DOI: 10.1081/SS-100100648
URL: http://dx.doi.org/10.1081/SS-100100648

PLEASE SCROLL DOWN FOR ARTICLE

Full terms and conditions of use: http://www.informaworld.com/terms-and-conditions-of-access.pdf

This article may be used for research, teaching and private study purposes. Any substantial or systematic reproduction, re-distribution, re-selling, loan or sub-licensing, systematic supply or distribution in any form to anyone is expressly forbidden.

The publisher does not give any warranty express or implied or make any representation that the contents will be complete or accurate or up to date. The accuracy of any instructions, formulae and drug doses should be independently verified with primary sources. The publisher shall not be liable for any loss, actions, claims, proceedings, demand or costs or damages whatsoever or howsoever caused arising directly or indirectly in connection with or arising out of the use of this material.

SEPARATION SCIENCE AND TECHNOLOGY, **34**(2), pp. 243–261, 1999

Modeling Concentration Polarization Phenomena for Shell-Side Flow in Ultrafiltration Process

SERGEI P. AGASHICHEV
DEPARTMENT OF CHEMICAL ENGINEERING
MENDELEJEV UNIVERSITY
MIUSSKAJA SQ. 9, MOSCOW A-47, RUSSIA 125047

Downloaded At: 11:16 25 January 2011

ABSTRACT

A correlation for the longitudinal mass flow of a dissolved component in terms of the degree of concentration polarization has been developed. The solution developed is applicable to shell-side flow and is based on the assumptions that the flow is to be isothermal, laminar, incompressible, and steady-state. Balance equations for viscous and diffusion boundary layers are the core of the model. Integration of these equations over the control volume of a hexagonal configuration has been carried out. This model permits analysis of the influence of mass flow, bulk concentration, velocity, and channel geometry on the degree of concentration polarization. In addition, it can give the mass flow by using the degree of concentration polarization as an input variable. The solution presented can be segmented and built into a complicated algorithm of a membrane-based process. The solution does not contain digital integration and permits simulation and analysis of the influence of various factors. Calculated data are included.

Key Words. Concentration polarization; Ultrafiltration; Modeling

INTRODUCTION

In recent years engineering and commercial interests have increasingly taken into consideration low-energy consuming and environmentally friendly processes. In this regard, membrane methods continue to have a wide spectrum of potential applications for solving ecological and industrial problems. Current trends reinforce the industrial potential of membrane-based technologies. In this respect the level of scientific interest in the engineering back-

Copyright © 1999 by Marcel Dekker, Inc. www.dekker.com

ORDER REPRINTS

ground of membrane technologies, in particular ultrafiltration, is expected to rise. There is a wide range of approaches to the calculation and design of the process. Some engineering solutions are hampered by the fact that many underlying mathematical models are based on unjustifiable simplifications and controversial assumptions. These include 1) isolated calculation of feed and permeate flow; 2) implication of the momentum balance equation without quantifying variation of longitudinal flow, etc. In this regard, development of an algorithm based on more justified physical premises and correct mathematical formulations is a central issue for modeling membrane operations.

FORMULATION OF THE PROBLEM

Ultrafiltration is accompanied by a phenomenon commonly referred to as concentration polarization (CP). The underlying mechanism for the concentration polarization phenomenon is unbalanced transport of dissolved components between the bulk and the membrane surface. In particular, convective flux toward the membrane surface is prevalent over backdiffusion to the bulk (see Fig. 2 below). The phenomenon has influenced process characteristics and has to be taken into consideration by modeling. The CP phenomenon is quantified by the degree of concentration polarization (or the ratio of the difference between surface and bulk concentration to bulk concentration). Empirical identification of the degree of concentration polarization requires the use of a rather cumbersome procedure. In this context a model-based approach is preferable.

Submodels for variation of driving force, transmembrane flux, and CP degree along the membrane surface are the core of any algorithm. For modeling longitudinal distribution of these variables, an analytical submodel for longitudinal flow in terms of parameters of hydrodynamic (U_{MAX}) and concentration (C_1, α) fields has to be developed. In addition, the submodel should reflect the geometrical configuration of the channel. Various approaches toward modeling the CP phenomenon have been presented (1–5). Modeling shell-side flow is hampered by the sophisticated configuration of the channel where mathematical formulation of the hydrodynamic and concentration fields requires a more complicated technique. A mathematical formulation of the CP phenomenon in analytical form for shell-side flow has not been found in the literature.

This article focuses on modeling the concentration polarization in the shell-side flow of the tubular unit in UF processes. It covers the development of a submodel for longitudinal mass flow in terms of parameters of concentration and hydrodynamic field. The submodel developed has to be segmented and built into an overall algorithm for calculation of the driving force, the transmembrane flux, and the CP degree along the membrane surface.

Downloaded At: 11:16 25 January 2011

Copyright © Marcel Dekker, Inc. All rights reserved.

MARCEL DEKKER, INC.
270 Madison Avenue, New York, New York 10016

ORDER REPRINTS

The general equation for the longitudinal flow rate of a dissolved component, M_{LONG1}, can be expressed mathematically as

$$\dot{M}_{\mathrm{LONG1}} = \iint_F u(r, \varphi) \cdot c(r, \varphi) \cdot dF \tag{1}$$

where $u(r, \varphi)$ is the axial velocity field in the shell-side; $c(r, \varphi)$ is the concentration field in the shell-side; r and φ are the radial and angular coordinates, respectively; and $dF = r \cdot dr \cdot d\varphi$ is the control surface normal to the axial coordinate. For an analytical solution to be developed, the input approximation for the hydrodynamic and concentration fields should be incorporated into Eq. (1).

UNDERLYING PREMISES AND ASSUMPTIONS OF THE MODEL

Consider a hexagonal membrane array. Select the control volume (triangular prism) restricted by symmetry planes (*ab*, *ad*, *cd*). The lines of intersection with the figure plane are shown in Fig. 1. The equations have to be written

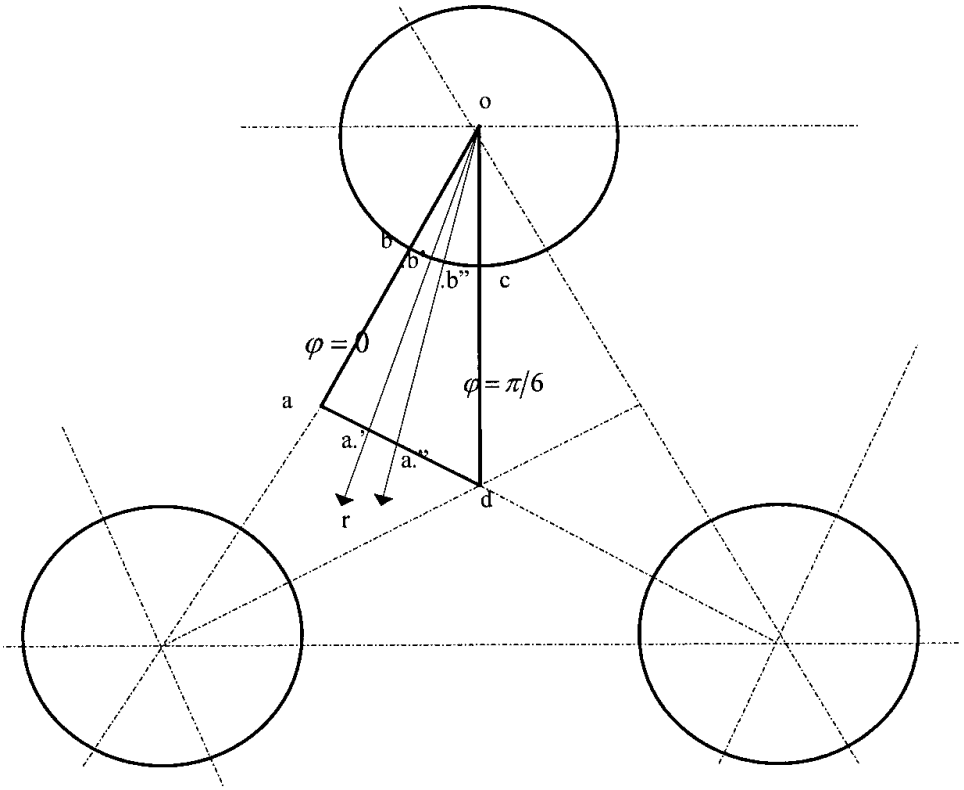

FIG. 1 Control volume (cross section of hexagonal membrane array).

Downloaded At: 11:16 25 January 2011

Copyright © Marcel Dekker, Inc. All rights reserved.

ORDER REPRINTS

over the elementary control volume. Further mathematical treatment is based on the following underlying assumptions.

- There is no mass transfer across symmetry planes. The intersection of the symmetry plane with the figure plane is shown in Fig. 1.
- The distance between the membrane surface and symmetry plane of the channel is assumed to be equal to the hydrodynamic boundary layer $\delta_W = f(\varphi)$, which depends on angular coordinate φ.
- The flow is assumed to be fully developed so the boundary layer thickness (δ_W), which is constant along the membrane surface, can be taken as the distance between the membrane surface and symmetry plane ''*ad*,'' which, in turn, depends on the angular coordinate φ. (See Fig. 1.)
- This article covers laminar flow. [Since the CP phenomenon is normally minimized in turbulent flow, some authors (5, 6) also state that it is the laminar regime that is preferable from the standpoint of energy consumption.]
- The flow is assumed to be incompressible, continuous, isothermal, and steady-state.

To solve Eq. (1), the integrand has to be nondimensionalized. A similar approach was used by modeling temperature polarization in membrane distillation processes (7). For this purpose we introduce the following dimensionless independent variables.

The first dimensionless distance coordinate, η, is the ratio of the current distance between the membrane surface and the symmetry plane (the scale unit is the distance between the membrane and the symmetry plane)

$$\eta = (r - R)/(Rn/\cos\varphi - R) \tag{2}$$

The coordinate η varies from $\eta_{r=R} = 0$ to $\eta_{r=Rn/\cos\varphi} = 1$.

The unit of scale in the η coordinate is equal to the distance from the membrane surface to the symmetry plane. It is assumed to be equal to the thickness of the current hydrodynamic layer, δ_W. The unit of scale, $(Rn/\cos\varphi - R) = \delta_W(\varphi)$, depends on the angular coordinate φ. It varies from $(Rn - R)$ when $\varphi = 0$ to $[Rn/\cos(\pi/6) - R]$ when $\varphi_{max} = \pi/6$. (It is visualized by the variable segments *ab*, *a′b′*, *a″b″* in Fig. 1.) The η coordinate is introduced to describe the hydrodynamic field. The velocity profile is expressed in terms of the η coordinate.

The second dimensionless coordinate, θ, is introduced to describe the profiles within the diffusion layer between $r = R$ and $r = R + \delta_C$. The scale unit in the θ coordinate is the concentration boundary layer thickness (f) in the η coordinate.

$$\theta = \eta/f = [—] \tag{3}$$

According to Schlichting (8), the ratio of diffusion (δ_C) to the hydrodynamic (δ_W) boundary layer can be estimated as

Downloaded At: 11:16 25 January 2011

Copyright © Marcel Dekker, Inc. All rights reserved.

MARCEL DEKKER, INC.
270 Madison Avenue, New York, New York 10016

ORDER REPRINTS

$$\delta_C/\delta_W = Sc^{-1/3} \tag{4}$$

Using the Ratio (4), the η coordinate can be correlated against the θ coordinate as

$$\theta = \sqrt[3]{Sc \cdot \eta} \tag{5}$$

Expressions (3) and (5) give $\theta = 0$ at the membrane surface when $\eta = 0$ ($r = R$). The upper boundary of diffusion layer, when $\eta = f = (Sc^{-1/3})$, gives $\theta = 1$ (see Fig. 2).

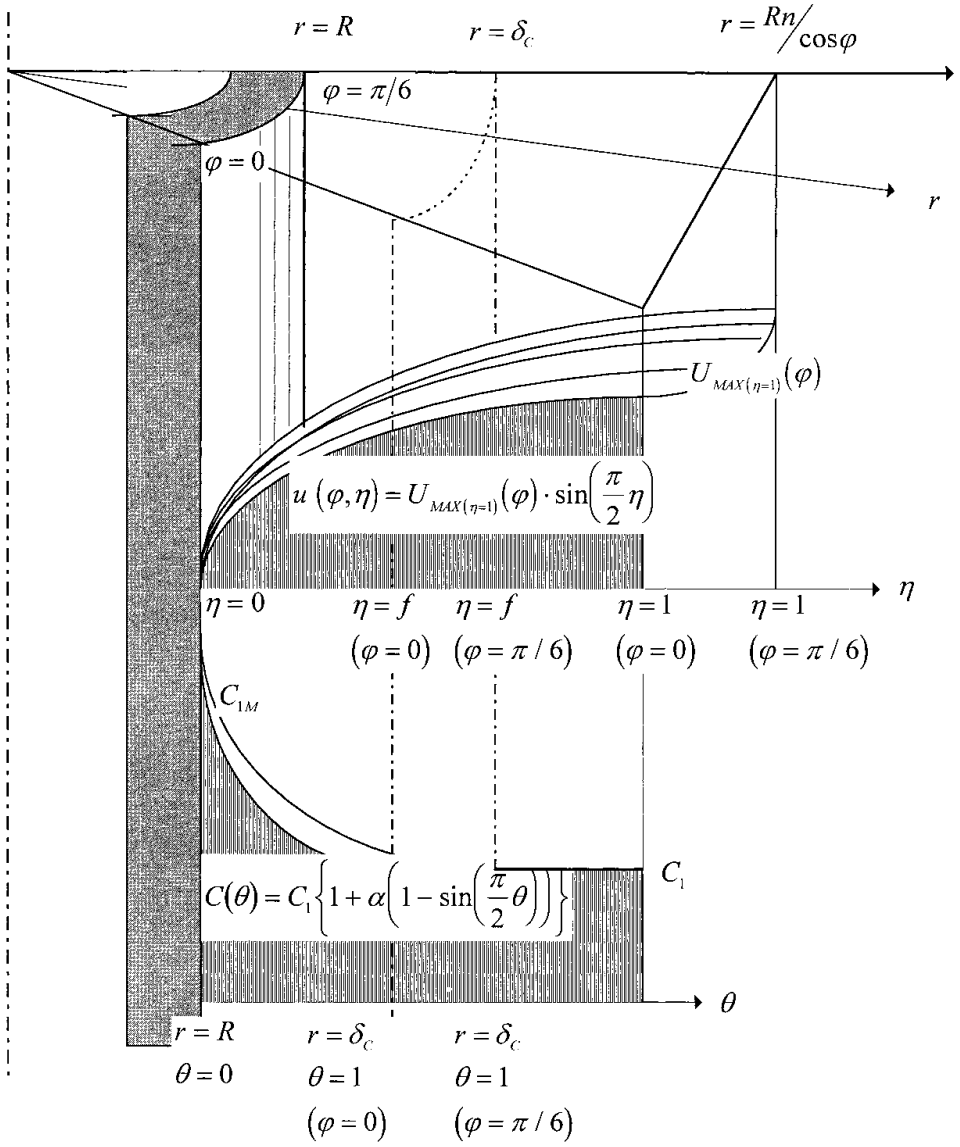

FIG. 2 Two-dimensional visualization of hydrodynamic and concentration field.

Downloaded At: 11:16 25 January 2011

Copyright © Marcel Dekker, Inc. All rights reserved.

ORDER REPRINTS

Hydrodynamic field. Some authors (8, 9) compare various approximations for the velocity profile as represented by polynomial, exponential, and sine wave (sinusoidal) functions. A sinusoidal curve corresponds to the shape of the physical profile and can be treated without using complicated mathematical techniques. In this regard a fragment of a sinusoidal function can be selected as a physically justifiable and mathematically preferable approximation. The shell-side control volume (Fig. 1) can be subdivided into a *set of elementary radial* fragments restricted by the symmetry plane, the membrane surface, and arbitrary radial cross sections with angular coordinates φ and $\varphi + d\varphi$. Flow in any radial fragment can be at least quantitatively similar to flow over a flat plate. For simplification of further mathematical treatment, flow is assumed to be approximated by a similar function at any angular coordinate.

Assuming the similarity of radial hydrodynamic projections at any value of angular coordinate, it is the maximum velocity that depends on the angular argument. The hydrodynamic field can be expressed as

$$u(\eta, \varphi) = U_{\mathrm{MAX}}(\varphi)\cdot\sin\left(\frac{\pi}{2}\,\eta\right) \tag{6}$$

The boundary conditions at the membrane surface are

$$u_{(\eta=0,\varphi=0)} = 0, \qquad u_{(\eta=0,\varphi=\pi/6)} = 0$$

and at the symmetry plane *ad* (see Fig. 1):

$$u_{(\eta=1,\varphi=0)} = U_{\mathrm{MAX}(\varphi=0)}, \qquad u_{(\eta=1,\varphi=\pi/6)} = U_{\mathrm{MAX}(\varphi=\pi/6)}$$

Figure 3 gives the current velocity profile in any arbitrary radial cross section. The upper boundary of the computational domain in dimensional representation, being dependent upon angular coordinates, varies from $r_{\mathrm{MAX}(\varphi=0)} = Rn/\cos(\varphi = 0)$ to $r_{\mathrm{MAX}(\gamma=\pi/6)} = Rn/\cos(\varphi = \pi/6)$, while in η coordinates the domain covers a range from $\eta = 0$ to $\eta = 1$ under any value of angular coordinate φ. The maximum velocity $U_{\mathrm{MAX}}(\varphi)$, as a function of angular coordinate φ, can be expressed assuming a similarity of hydrodynamic profiles in any radial cross sections [*ab*, *a′b′*, *a″b″* (see Fig. 1)] as follows:

$$\frac{U_{\mathrm{MAX}(\eta=1)}(\varphi)}{U_{\mathrm{MAX}(\eta=1,\varphi=\pi/6)}} = \frac{(n/\cos\,\varphi - 1)}{(n/\cos\{\pi/6\} - 1)} \tag{7}$$

The maximum velocity (when $\eta = 1$) under any current angular coordinate φ becomes

$$U_{\mathrm{MAX}(\eta=1)}(\varphi) = \frac{U_{\mathrm{MAX}(\eta=1,\varphi=\varphi/6)}}{(n/\cos\{\pi/6\} - 1)}\,(n/\cos\,\varphi - 1) \tag{8}$$

Figure 4 gives a graphical visualization of U_{MAX} as a function of angular coordinate φ under various densities of the membrane bundle (n).

Downloaded At: 11:16 25 January 2011

Copyright © Marcel Dekker, Inc. All rights reserved.

MARCEL DEKKER, INC.
270 Madison Avenue, New York, New York 10016

ORDER REPRINTS

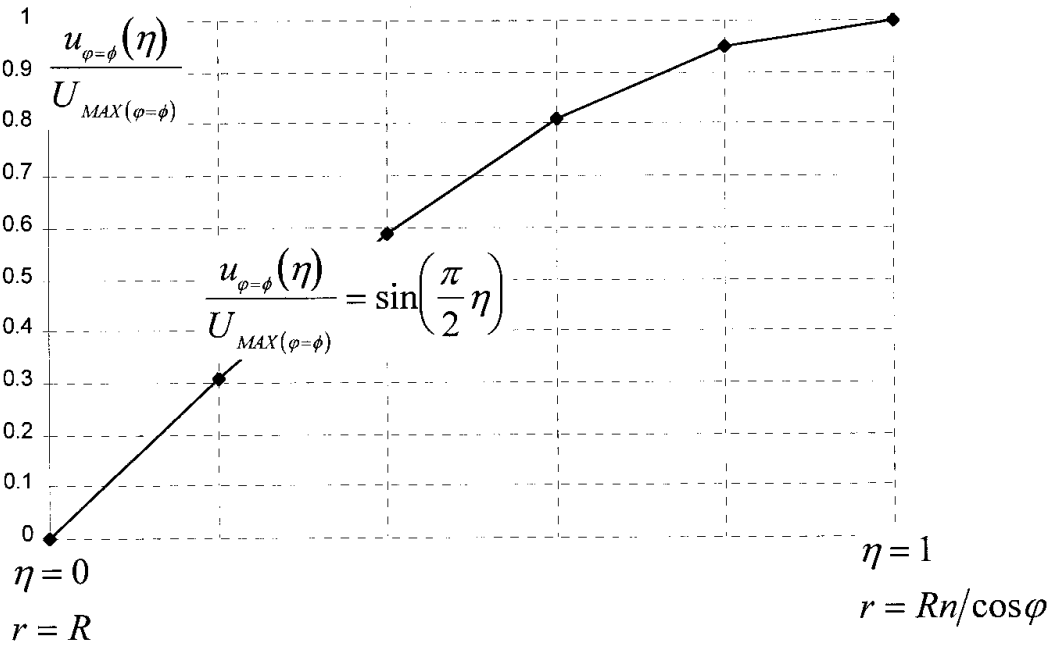

FIG. 3 One-dimensional projection of hydrodynamic profile against dimensionless radial variable η under arbitrary value of angular argument φ.

$$[X] = \eta, \qquad [Y] = \frac{u_{\varphi=\phi}(\eta)}{U_{\mathrm{MAX}(\varphi=\phi)}}$$

Incorporating the expression for maximum velocity $U_{\mathrm{MAX}}(\varphi)$ into Eq. (6), the hydrodynamic field can be written with respect to φ and η variables as follows:

$$u(\eta, \varphi) = U_{\mathrm{MAX}(\eta=1,\varphi=\pi/6)} \frac{(n/\cos\varphi - 1)}{(n/\cos\{\pi/6\} - 1)} \cdot \sin\left(\frac{\pi}{2}\eta\right) \tag{9}$$

With respect to the θ coordinate, Eq. (9) can be rewritten as

$$u(\theta, \varphi) = U_{\mathrm{MAX}(\eta=1,\varphi=\pi/6)} \frac{(n/\cos\varphi - 1)}{(n/\cos\{\pi/6\} - 1)} \cdot \sin\left(\frac{\pi}{2} f\theta\right) \tag{10}$$

Concentration field. Membrane separation is accompanied by an unavoidable phenomenon commonly referred to as concentration polarization. CP is caused by the unbalanced transport of a dissolved component between the bulk and the membrane surface, in particular a convective flux toward the membrane surface is prevalent over backdiffusion transport to the bulk. It increases the concentration at the membrane surface. To quantify the CP phenomenon we selected a sine wave profile similar to the hydrodynamic

Downloaded At: 11:16 25 January 2011

Copyright © Marcel Dekker, Inc. All rights reserved.

ORDER REPRINTS

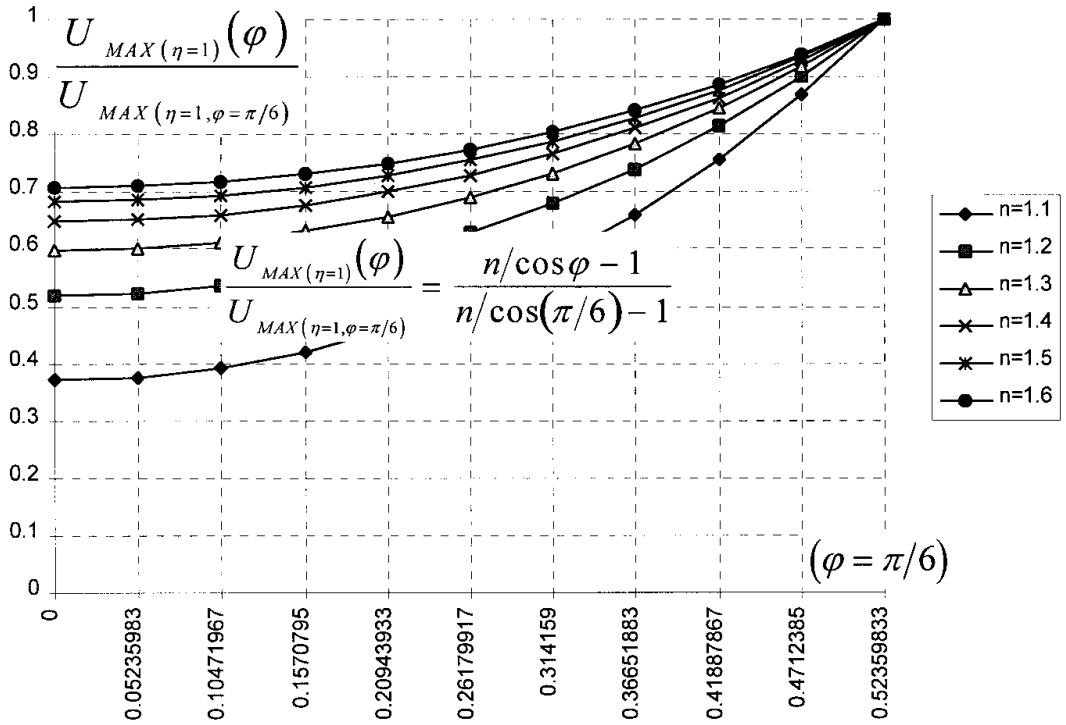

FIG. 4 Maximum velocity (at the symmetry plane) in dimensionless form against angular coordinate φ under various densities of membrane bundle (n).

$$[X] = \varphi, \qquad [Y] = \frac{U_{\mathrm{MAX}(\eta=1)}(\varphi)}{U_{\mathrm{MAX}(\eta=1,\varphi=\pi/6)}}$$

one. This profile was selected for convenience and was not derived from underlying physics. In dimensionless representation (with respect to the coordinate θ), the radial distribution of concentration is expressed as

$$\frac{c(\theta) - C_1}{C_{1\mathrm{M}} - C_1} = 1 - \sin\left(\frac{\pi}{2}\theta\right) \tag{11}$$

Boundary conditions at the membrane surface are

$$c_{(\theta=0,\varphi=0)} = C_{1\mathrm{M}}, \qquad c_{(\theta=0,\varphi=\pi/6)} = C_{1\mathrm{M}}$$

and at the centerline are

$$c_{(\theta=1,\varphi=0)} = C_1, \qquad c_{(\theta=1,\varphi=\pi/6)} = C_1$$

Downloaded At: 11:16 25 January 2011

Copyright © Marcel Dekker, Inc. All rights reserved.

MARCEL DEKKER, INC.
270 Madison Avenue, New York, New York 10016

ORDER REPRINTS

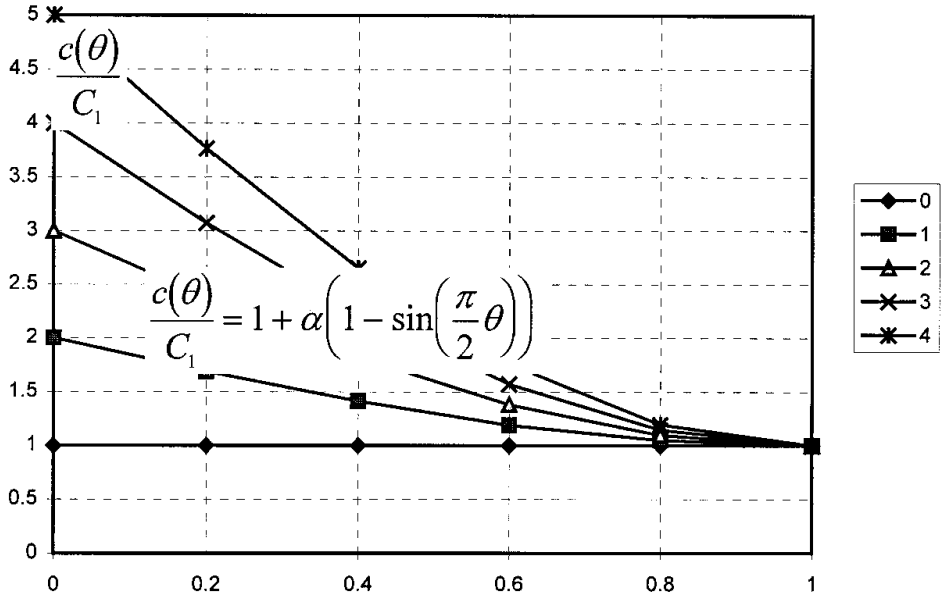

FIG. 5 Set of radial projections of concentration field under various degrees of concentration polarization (α).

$$[X] = \theta, \qquad [Y] = \frac{c(\theta)}{C_1} = 1 + \alpha\left[1 - \sin\left(\frac{\pi}{2}\theta\right)\right]$$

In terms of degree of concentration polarization (α), Eq. (11) gives

$$c(\theta) = C_1 \cdot \left\{1 + \alpha\cdot\left(1 - \sin\left(\frac{\pi}{2}\theta\right)\right)\right\} \tag{12}$$

where $\alpha = (C_{1M} - C_1)/C_1$.

Figure 5 gives a set of radial projections of the concentration field under various degrees of α. A two-dimensional visualization of hydrodynamic and the concentration fields is given in Fig. 2.

MODELING THE LONGITUDINAL MASS FLOW RATE AS A FUNCTION OF THE DEGREE OF CONCENTRATION POLARIZATION

This section focuses on correlation of the flow rate of a dissolved component (m) against the parameters of the concentration and hydrodynamic field, viz., bulk velocity and concentration (U_1, C_1), membrane surface concentration (C_{1M}), or degrees of α and boundary layer thickness (f).

Downloaded At: 11:16 25 January 2011

Copyright © Marcel Dekker, Inc. All rights reserved.

ORDER REPRINTS

For the quantitative estimation of the profile of transmembrane flux with respect to the axial coordinate to be developed, the correlation of mass flow against the degree of CP should be developed. Equation (1) gives a general mathematical expression for the mass flow rate, taking into consideration the simplifying assumptions and geometry of control volume. The right-hand side of Eq. (1) can be rewritten as a double integral in polar coordinates, with variable radial upper limits (see Fig. 2):

$$\dot{M}_{\mathrm{LONG1}} = \int_{\varphi=0}^{\varphi=\pi/6} \left(\int_{r=R}^{r=Rn/\cos\varphi} u(r\varphi) \cdot c(r) \cdot r \cdot dr \right) \cdot d\varphi \qquad (13)$$

The inner integral, which is the first to be evaluated with respect to the radial coordinate, is restricted by limits R and $Rn/\cos\varphi$. The outer integral, with respect to the angular coordinate, has angular limits $\varphi = 0$ and $\varphi = \pi/6$.

For simplification of mathematical treatment, the computational domain has to be subdivided into two zones (see Fig. 2). The first one (Zone A) lies between $r = R$ and $r = R + \delta_C$ and belongs to the diffusion boundary layer. Within the first zone there is radial and angular variation of both concentration and velocity. The second one (Zone B) is restricted by the upper boundary of the diffusion layer and the symmetry plane of the channel. Within the second zone there are radial and angular variation of velocity while the concentration remains constant (equal to C_1). In this regard, Eq. (13) gives two terms on the right-hand side.

$$\begin{aligned} \dot{M}_{\mathrm{LONG1}} &= \int_{\varphi=0}^{\varphi=\pi/6} \left(\int_{r=R}^{r=Rn/\cos\varphi} u(r\varphi) \cdot c(r\varphi) \cdot r \cdot dr \right) \cdot d\varphi \\ &= \int_{\varphi=0}^{\varphi=\pi/6} \left(\int_{r=R}^{r=R+\delta_C} u(r\varphi) \cdot c(r\varphi) \cdot r \cdot dr \right) \cdot d\varphi \\ &\quad + \int_{\varphi=0}^{\varphi=\pi/6} \left(\int_{r=R+\delta_C}^{r=Rn/\cos\varphi} u(r\varphi) \cdot C_1 \cdot r \cdot dr \right) \cdot d\varphi \end{aligned} \qquad (14)$$

Zone A. Consider the right-hand side of Eq. (14). The first term reflects flow of dissolved component within the diffusion boundary layer. Further mathematical treatment of this term has to be carried out with respect to the second dimensionless coordinate θ.

$$\dot{M}_{\mathrm{LONG1(A)}} = \int_{\varphi=0}^{\varphi=\pi/6} \left(\int_{\substack{(r=R)\\ \theta=0}}^{\substack{(r=R+\delta_C)\\ \theta=1}} u(r, \varphi) \cdot c(r) \cdot r \cdot dr \right) \cdot d\varphi \qquad (15)$$

Following integration, Eq. (15) gives

Downloaded At: 11:16 25 January 2011

Copyright © Marcel Dekker, Inc. All rights reserved.

ORDER REPRINTS

$$\dot{M}_{\mathrm{LONG(A)}} = C_1 U_{\mathrm{MAX}(\varphi=\pi/6)} \mathbf{D}_{\mathrm{A}} \tag{16}$$

where a 1×1 matrix, $\mathbf{D}_{\mathrm{A}}$, is the product of a raw matrix, $\mathbf{K}_{\mathrm{A}}$, and a column matrix, $\mathbf{G}$ (see Appendix A).

Zone B lies between the upper boundary of the concentration layer and the symmetry plane of the channel (see Fig. 2). The second term on the right-hand side of Eq. (14) reflects the flow within Zone B where there is variation of velocity while the concentration remains constant (equal to C_1). To simplify the mathematical treatment, the input correlation has to be written with respect to the η variable

$$\dot{M}_{\mathrm{LONG(B)}} = \int_{\varphi=0}^{\varphi=\pi/6} d\varphi \int_{r=R+\delta_{\mathrm{C}}}^{r=Rn/\cos\varphi} u(r\varphi) \cdot c_1 \cdot r \cdot dr \tag{17}$$

Following integration, Eq. (17) gives

$$\dot{M}_{\mathrm{LONG(B)}} = C_1 U_{\mathrm{MAX}(\varphi=\pi/6)} \mathbf{D}_{\mathrm{B}} \tag{18}$$

where a 1×1 matrix, $\mathbf{D}_{\mathrm{B}}$, is the product of a raw matrix, $\mathbf{K}_{\mathrm{B}}$, and a column matrix, $\mathbf{G}$ (see Appendix B).

Dividing the developed mass flow expressions (Eqs. 16 and 18) by the cross section of shell-side flow, we have

$$\begin{aligned} \dot{m}_{\mathrm{LONG}}(\alpha) &= \frac{\dot{M}_{\mathrm{LONG(A)}} + \dot{M}_{\mathrm{LONG(B)}}}{F_{\mathrm{SHELL}}} \\ &= \frac{U_{\mathrm{MAX}(\varphi=\pi/6)} \cdot C_1}{F_{\mathrm{SHELL}}} (\mathbf{D}_{\mathrm{A}} + \mathbf{D}_{\mathrm{B}}) \end{aligned} \tag{19}$$

where the cross section of the shell-side flow is

$$F_{\mathrm{SHELL}} = (\sqrt{3}n^2/8 \cos^2(\pi/6) - \pi/12) \cdot R^2 \tag{20}$$

$\mathbf{D}_{\mathrm{A}}$ and $\mathbf{D}_{\mathrm{B}}$ are from Eqs. (A5) and (B4), respectively (see Appendixes A and B).

IMPLICATION OF THE MODEL

A model giving a quantitative relationship between mass flow and the parameters of hydrodynamic and concentration fields can be built into a more complicated algorithm. A simplified fragment of the algorithm can be described as follows: A preliminarily mass flow rate (m) calculated from the balance equation has to be inserted into Eq. (19) which has to be solved for the degree of α, where the input data are the axial velocity (U_{MAX}), the bulk concentration (C_1), the density of the membrane array (n), and the outer

Downloaded At: 11:16 25 January 2011

Copyright © Marcel Dekker, Inc. All rights reserved.

ORDER REPRINTS

TABLE 1
Mass Flow of Dissolved Component (m_{LONG}) under Various Degrees of Concentration Polarization (α) and Concentration Layer Thickness (f), where m_{LONG} = [kg/m^2 − s], $f = \delta_C/\delta_W$ = [—], $\alpha = (C_{1M} - C_1)/C_1$ = [—]. Input data: U_{MAX} = 1 m/s, C_1 = 10 kg/m^3·n = 1.1 [—]

	f = 0	f = 0.1	f = 0.2	f = 0.3	f = 0.4	f = 0.5
α = 0	4.13345	4.20216	4.27094	4.33972	4.40849	4.47727
α = 1	4.13352	4.35437	4.74425	5.30261	6.02431	6.89949
α = 2	4.13359	4.50658	5.21755	6.26549	7.64013	9.32172
α = 3	4.13366	4.65878	5.69086	7.22838	9.25595	11.7439
α = 4	4.13373	4.81099	6.16417	8.19127	10.8718	14.1662
	f = 0.6	f = 0.7	f = 0.8	f = 0.9	f = 1	
α = 0	4.54605	4.61482	4.6836	4.75238	4.82046	
α = 1	7.91363	9.04783	10.2791	11.5811	12.9108	
α = 2	11.2812	13.4808	15.8747	18.4098	21.0011	
α = 3	14.6488	17.9138	21.4702	25.2386	29.0914	
α = 4	18.0164	22.3469	27.0658	32.0673	37.1817	

Downloaded At: 11:16 25 January 2011

membrane's radius (R). The thickness of the diffusion layer, f, is assumed to be equal to $Sc^{-1/3}$ (Eq. 4).

Calculated data on the mass flow rate against the value of the diffusion layer under various degrees of concentration polarization and the density of the membrane array are presented in Table 1 and visualized in Fig. 6. By analyzing calculated data, one can conclude that the increase of the CP degree and the boundary layer thickness will cause the growth of a longitudinal flow that does not contradict the underlying physics.

When experimental data on the mass balance are available, the model permits analysis of the degree of concentration polarization along the membrane surface. The model does not contain digital integration, which makes it attractive for modeling complicated membrane-based processes. The algorithm presented can be used as an alternative to modeling operations on a hollow fiber unit where fluctuation of the individual fibers is negligible. The developed submodel could be applied to modeling mass transfer in thermomembrane operations as well.

CONCLUSIONS

The developed model permits quantitative correlation of longitudinal mass flow against the degree of concentration polarization. The submitted model enables analysis of the influence of mass flow (m), bulk concentration (C_1),

Copyright © Marcel Dekker, Inc. All rights reserved.

MARCEL DEKKER, INC.
270 Madison Avenue, New York, New York 10016

ORDER REPRINTS

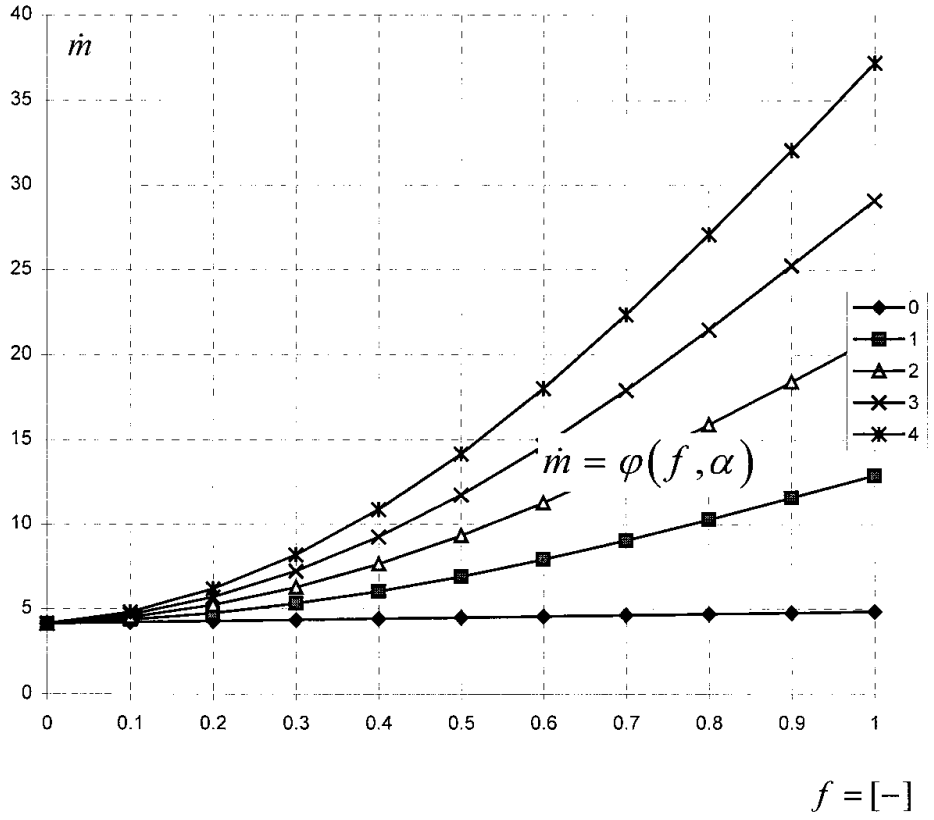

FIG. 6 Mass flow of dissolved component (m_{LONG}) vs concentration layer thickness (f) under various degrees of concentration polarization (α), where m_{LONG} = [kg/m^2 − s], $f = \delta_C/\delta_W$ = [—], $\alpha = (C_{1M} - C_1)/C_1$ = [—]. Input data: U_{MAX} = 1 m/s, C_1 = 10 kg/m^3·n = 1.1 [—].

$$[X] = f = [—], \qquad [Y] = m_{LONG} = [kg/m^2 - s]$$

axial velocity (U_{MAX}) and channel geometry (n, R) on the degree of concentration polarization (α). It can also give mass flow by using the degree of concentration polarization as an input variable. The developed model is going to be segmented and built into a complicated algorithm for longitudinal calculation of the following variables: concentration polarization, driving force, and transmembrane flux.

APPENDIX A: INTEGRATING EQ. (15) OVER THE DIFFUSION BOUNDARY LAYER (ZONE A)

Zone A covers the area between $r = R$ and $r = R + \delta_C$. It belongs to the diffusion boundary layer where there is radial and angular variation of both concentration and velocity. Equation (15) reflects the flow of a dissolved component within it. Further mathematical treatment of this term has to be carried out with respect to the second dimensionless coordinate θ.

Downloaded At: 11:16 25 January 2011

Copyright © Marcel Dekker, Inc. All rights reserved.

ORDER REPRINTS

$$\dot{M}_{\mathrm{LONG1(A)}} = \int_{\varphi=0}^{\varphi=\pi/6} \left(\int_{\substack{(r=R)\\ \theta=0}}^{\substack{(r=R+\delta_C)\\ \theta=1}} u(r, \varphi) \cdot c(r, \varphi) \cdot r \cdot dr \right) \cdot d\varphi \quad \text{(A1)}$$

All input functions in terms of the second dimensionless coordinate θ are given below.

$$\text{Where } u(\theta, \varphi) = U_{\mathrm{MAX}(\eta=1)}(\varphi) \cdot \sin\left(\frac{\pi}{2} f\theta\right) \text{ from Eq. (10)}$$

$$U_{\mathrm{MAX}(\eta=1)}(\varphi) = U_{\mathrm{MAX}(\eta=1,\varphi=\pi/6)} \cdot \frac{(n/\cos\varphi - 1)}{(n/\cos\{\pi/6\} - 1)} \text{ from Eq. (8)}$$

$$c(\theta) = C_1 \cdot \left\{1 + \alpha \cdot \left(1 - \sin\left(\frac{\pi}{2}\theta\right)\right)\right\} \text{ from Eq. (12):}$$

$$dF_{\mathrm{A}}(\theta, \varphi) = rdrd\varphi = R^2[1 + (n/\cos\varphi - 1)f\theta][n/\cos\varphi - 1]fd\theta d\varphi \quad \text{(A2)}$$

where the expressions for r and dr in terms of the θ variable are taken from Eqs. (2) and (3). Incorporating correlations for the hydrodynamic (Eq. 10) and concentration (Eq. 12) profiles, Eq. (A1) gives

$$\dot{M}_{\mathrm{LONG(A)}} = \int_{\varphi=0}^{\varphi=\pi/6} d\varphi \int_{\substack{(r=R)\\ \theta=0}}^{\substack{(r=R+\delta_C)\\ \theta=1}} U_{\mathrm{MAX}}(\varphi) \cdot \sin\left(\frac{\pi}{2} f\theta\right) \cdot C_1\left\{1_1 + \alpha\left(1 - \sin\left(\frac{\pi}{2}\theta\right)\right)\right\} \cdot R^2(1 + (n/\cos\varphi - 1)f\theta) \cdot (n/\cos\varphi - 1) \cdot fd\theta \quad \text{(A3)}$$

Integrating Eq. (A3) over the control section with respect to a dimensionless radial and angular coordinates, we have the longitudinal flow of dissolved component $M_{\mathrm{LONG(A)}}$ in terms of geometry factor and process parameters. Intermediate expressions have been regrouped as elements of arrays. In matrix notation, it can be written as

$$\dot{M}_{\mathrm{LONG(A)}} = C_1 U_{\mathrm{MAX}(\varphi=\pi/6)} \mathbf{D}_{\mathrm{A}} \quad \text{(A4)}$$

where a 1×1 matrix, $\mathbf{D}_{\mathrm{A}}$, is the product of a raw matrix, $\mathbf{K}_{\mathrm{A}}$, and a column matrix, $\mathbf{G}$:

$$\mathbf{K}_{\mathrm{A}}\mathbf{G} = [k_{\mathrm{A}1}g_1 + k_{\mathrm{A}2}g_2 + k_{\mathrm{A}3}g_3 + k_{\mathrm{A}4}g_4] = \mathbf{D}_{\mathrm{A}} \quad \text{(A5)}$$

Column matrix $\mathbf{G}$ has the following elements:

Downloaded At: 11:16 25 January 2011

Copyright © Marcel Dekker, Inc. All rights reserved.

ORDER REPRINTS

$$g_1 = n^3R^2\left(\frac{\cos(\pi/6)}{n - \cos(\pi/6)}\right)\cdot F_1 \quad \text{(A6-1)}$$

$$g_2 = n^2R^2\left(\frac{\cos(\pi/6)}{n - \cos(\pi/6)}\right)\cdot F_2 \quad \text{(A6-2)}$$

$$g_3 = nR^2\left(\frac{\cos(\pi/6)}{n - \cos(\pi/6)}\right)\cdot F_3 \quad \text{(A6-3)}$$

$$g_4 = R^2\left(\frac{\cos(\pi/6)}{n - \cos(\pi/6)}\right)\cdot F_4 \quad \text{(A6-4)}$$

where the elements F_1–F_4 are obtained by outer integrating with respect to the angular coordinate *as* (for the hexagonal membrane array, the angular boundaries of integration are $\varphi = 0$ and $\varphi = \pi/6$). See Fig. 2.

$$F_1 = \int_{\varphi=0}^{\varphi=\pi/6} \frac{d\varphi}{\cos^3\varphi} = \frac{\sin(\pi/6)}{2\cdot\cos^2(\pi/6)} + 0.5\cdot\ln(tg(\pi/3)) \quad \text{(A7-1)}$$

$$F_2 = \int_{\varphi=0}^{\varphi=\pi/6} \frac{d\varphi}{\cos^2\varphi} = tg(\pi/6) \quad \text{(A7-2)}$$

$$F_3 = \int_{\varphi=0}^{\varphi=\pi/6} \frac{d\varphi}{\cos\varphi} = \ln(tg(\pi/3)) \quad \text{(A7-3)}$$

$$F_4 = \int_{\varphi=0}^{\varphi=\pi/6} d\varphi = \pi/6 \quad \text{(A7-4)}$$

Elements of the column matrix **G** depend on channel geometry, in particular the density of the membrane array (n), the outer radius of the tubular membrane (R), and the configuration of the intertubular channel (for a hexagonal array, $\varphi = \pi/6$; and for a square array, $\varphi = \pi/4$; etc. See Fig. 1).

The raw matrix, $\mathbf{K}_A$ (see Eq. A5), has the following subelements:

$$k_{A1} = f^2E_1 \quad \text{(A8-1)}$$

$$k_{A2} = -3f^2E_1 + fE_2 \quad \text{(A8-2)}$$

$$k_{A3} = 3f^2E_1 - 2fE_2 \quad \text{(A8-3)}$$

$$k_{A4} = -f^2E_1 + fE_2 \quad \text{(A8-4)}$$

where

$$E_1 = (\alpha + 1)\cdot I_3 - \alpha\cdot I_1\cdot \quad \text{(A9-1)}$$

$$E_2 = (\alpha + 1)\cdot I_4 - \alpha\cdot I_2\cdot \quad \text{(A9-2)}$$

where

Downloaded At: 11:16 25 January 2011

Copyright © Marcel Dekker, Inc. All rights reserved.

ORDER REPRINTS

$$I_1 = \frac{\sin Y}{2Y} - \frac{\sin X}{2X} + \frac{\cos X - 1}{2X^2} + \frac{1 - \cos Y}{2Y^2} \quad \text{(A10-1)}$$

$$I_2 = \frac{\sin Y}{2Y} - \frac{\sin X}{2X} \quad \text{(A10-2)}$$

$$I_3 = \frac{\sin B}{B^2} - \frac{\cos B}{B} \quad \text{(A10-3)}$$

$$I_4 = \frac{1 - \cos B}{B} \quad \text{(A10-4)}$$

where

$$X = A + B \quad \text{and} \quad Y = A - B \quad \text{(A11)}$$

$$A = \frac{\pi}{2} \quad \text{and} \quad B = \frac{\pi}{2} f \quad \text{(A12)}$$

where $f = \mathrm{Sc}^{-1/3}$ from Eq. (4).

Elements of the raw matrix $\mathbf{K}_A$ depend on concentration field variables, in particular the degree of concentration polarization (α) and the diffusion boundary layer thickness (f).

APPENDIX B: INTEGRATING EQ. (17) OVER THE AREA BETWEEN THE UPPER DIFFUSION BOUNDARY AND THE SYMMETRY PLANE OF THE CHANNEL (ZONE B)

Zone B lies between the upper boundary of the concentration layer and the symmetry plane of the channel (see Fig. 2). Equation (17) reflects the flow within Zone B where there is variation of velocity while the concentration remains constant (equal to C_1). To simplify the mathematical treatment, the input correlation has to be written with respect to the η variable:

$$\dot{M}_{\mathrm{LONG(B)}} = \int_{\varphi=0}^{\varphi=\pi/6} d\varphi \int_{r=R+\delta_C}^{r=Rn/\cos\varphi} u(r\varphi)\cdot c_1 \cdot r \cdot dr \quad \text{(B1)}$$

$$\text{Where } U(\eta, \varphi) = U_{\mathrm{MAX}(\eta=1)}(\varphi)\cdot\sin\left(\frac{\pi}{2}\eta\right) \text{ from Eq. (9)}$$

$$\text{where } U_{\mathrm{MAX}(\eta=1)}(\varphi) = U_{\mathrm{MAX}(\eta=1,\varphi=\pi/6)}\cdot\frac{(n/\cos\varphi - 1)}{(n/\cos\{\pi/6\} - 1)} \text{ from Eq. (8)}$$

$$dF_B(\eta, \varphi) = r dr d\varphi \quad \text{(B2)}$$

$$= [R + (Rn/\cos\varphi - R)\eta][Rn/\cos\varphi - R]d\eta d\varphi$$

Downloaded At: 11:16 25 January 2011

Copyright © Marcel Dekker, Inc. All rights reserved.

MARCEL DEKKER, INC.
270 Madison Avenue, New York, New York 10016

ORDER REPRINTS

By inserting input approximations with respect to η and φ variables, Eq. (B1) can be written as

$$\dot{M}_{\mathrm{LONG(B)}} = \int_{\varphi=0}^{\varphi=\pi/6} d\varphi \int_{\substack{\eta=f \\ (r=R+\delta_C)}}^{\substack{(r=Rn/\cos\varphi) \\ \eta=1}} \underset{(\eta=1)}{U_{\mathrm{MAX}}(\varphi)} \cdot \sin\left(\frac{\pi}{2}\,\eta\right) \cdot C_1 \cdot R^2[1 + (n/\cos\varphi - 1)\eta][n/\cos\varphi - 1] \cdot d\eta \tag{B3}$$

The inner integral, which is the first to be evaluated with respect to radial variable η, is restricted by limits $\eta = f$ and $\eta = 1$ (see Fig. 2). The outer integral with respect to the angular coordinate has limits $\varphi = 0$ and $\varphi = \pi/6$.

Integrating Eq. (B3) over Zone B with respect to angular coordinate φ and the first dimensionless coordinate η, we have

$$\dot{M}_{\mathrm{LONG(B)}} = C_1 U_{\mathrm{MAX}(\varphi=\pi/6)} \mathbf{D}_{\mathrm{B}} \tag{B4}$$

where a 1×1 matrix, $\mathbf{D}_{\mathrm{B}}$, is the product of a raw matrix, $\mathbf{K}_{\mathrm{B}}$, and a column matrix, $\mathbf{G}$.

Intermediate expressions have been presented in matrix notation as follows:

$$\mathbf{K}_{\mathrm{B}}\mathbf{G} = [k_{\mathrm{B1}}g_1 + k_{\mathrm{B2}}g_2 + k_{\mathrm{B3}}g_3 + k_{\mathrm{B4}}g_4] = \mathbf{D}_{\mathrm{B}} \tag{B5}$$

where

$$k_{\mathrm{B1}} = I_6 \tag{B6a}$$

$$k_{\mathrm{B2}} = I_5 - 3I_6 \tag{B6b}$$

$$k_{\mathrm{B3}} = -2I_5 + 3I_6 \tag{B6c}$$

$$k_{\mathrm{B4}} = I_5 - I_6 \tag{B6d}$$

where

$$I_5 = \frac{\cos B}{A} \tag{B7}$$

$$I_6 = f \cdot \frac{\cos B}{A} + \frac{1 - \sin B}{A^2} \tag{B8}$$

where

$$A = \frac{\pi}{2} \quad \text{and} \quad B = \frac{\pi}{2} f \tag{B9}$$

and where $f = \mathrm{Sc}^{-1/3}$ from Eq. (4).

Downloaded At: 11:16 25 January 2011

Copyright © Marcel Dekker, Inc. All rights reserved.

MARCEL DEKKER, INC.
270 Madison Avenue, New York, New York 10016

ORDER REPRINTS

SYMBOLS

C_1	bulk concentration of dissolved component (kg/m^3)
C_{1M}	concentration of dissolved component at membrane surface (kg/m^3)
D	diffusivity (m^2/s)
F	surface (m^2)
f	dimensionless diffusion layer thickness ($f = \delta_C/\delta_W$) (—)
$\dot{M}$	mass flow rate of dissolved component (kg/s)
$\dot{m}$	mass flow rate of dissolved component per square meter (kg/m^2·s)
n	ratio of intertubular distance to membrane's outer diameter (—)
r	current radial coordinate (m)
R	outer membrane's radius (m)
Sc	Schmidt number, Sc $= \mu/D\rho$
$u(r, \varphi)$, $u(\eta, \varphi)$, etc., (U_{MAX})	current (axial) velocity (m/s)
α	degree of concentration polarization, $\alpha = (C_{1M} - C_1)/C_1$ (—)
δ_C	diffusion layer height (m)
δ_W	hydrodynamic layer height (m)
μ	dynamic viscosity (Pa·s)
η	first dimensionless distance coordinate ($\eta = (r - R)/(Rn/\cos\varphi - R)) = (—)$
ρ	density (kg/m^3)
θ	second dimensionless distance coordinate ($\theta = \eta/f) = (—)$
φ	angular coordinate

Subscripts

1	corresponds to the bulk parameter
1M	corresponds to the membrane surface parameter
LONG	longitudinal

REFERENCES

1. C. Kleinstreuer and M. S. Paller, ''Laminar Dilute Suspension Flows in Plate-and-Frame Ultra Filtration Units,'' *AIChE J.*, *29*(4) (1983).

Downloaded At: 11:16 25 January 2011

Copyright © Marcel Dekker, Inc. All rights reserved.

MARCEL DEKKER, INC.
270 Madison Avenue, New York, New York 10016

ORDER REPRINTS

2. M. Sekino, ''Study of an Analytical Model for Hollow Fibre Reverse Osmosis Module Systems,'' *Desalination*, *100*, 85–97 (1995).
3. R. Rautenbach and R. Albrecht, *Membrane Process*, Wiley, New York, NY, 1989.
4. W. S. W. Ho and K. K. Sirkar, *Membrane Handbook*, Van Nostrand, New York, NY, 1992.
5. R. F. Madsen, *Hyperfiltration and ultrafiltration in Plate-and-Frame Systems*, Elsevier Scientific, Amsterdam, 1977.
6. M. C. Porter, ''The Effect of Fluid Management on Membrane Filter Throughput,'' in *Proceedings of 2nd Pacific Chemical Engineering Congress*, *New York*, *1977*, *Vol. 2*(4), pp. 975–982.
7. S. Agashichev and V. Falalejev, ''Modelling Temperature Polarisation Phenomenon for Longitudinal Shell-Side Flow in Membrane Distillation Process,'' *Desalination*, *108*, 99–103 (1996).
8. H. Schlichting, *Grenzschicht-Theorie*, 5th ed., Verlag G. Braun, Karlsruhe, 1974.
9. P. M. Gerhart, R. J. Gross, and J. I. Hochstein, *Fundamentals of Fluid Mechanics*, Addison-Wesley, Reading, MA, 1992.

Received by editor October 21, 1997
Revision received May 1998

Downloaded At: 11:16 25 January 2011

Copyright © Marcel Dekker, Inc. All rights reserved.

MARCEL DEKKER, INC.
270 Madison Avenue, New York, New York 10016

Downloaded At: 11:16 25 January 2011

Request Permission or Order Reprints Instantly!

Interested in copying and sharing this article? In most cases, U.S. Copyright Law requires that you get permission from the article's rightsholder before using copyrighted content.

All information and materials found in this article, including but not limited to text, trademarks, patents, logos, graphics and images (the "Materials"), are the copyrighted works and other forms of intellectual property of Marcel Dekker, Inc., or its licensors. All rights not expressly granted are reserved.

Get permission to lawfully reproduce and distribute the Materials or order reprints quickly and painlessly. Simply click on the "Request Permission/Reprints Here" link below and follow the instructions. Visit the U.S. Copyright Office for information on Fair Use limitations of U.S. copyright law. Please refer to The Association of American Publishers' (AAP) website for guidelines on Fair Use in the Classroom.

The Materials are for your personal use only and cannot be reformatted, reposted, resold or distributed by electronic means or otherwise without permission from Marcel Dekker, Inc. Marcel Dekker, Inc. grants you the limited right to display the Materials only on your personal computer or personal wireless device, and to copy and download single copies of such Materials provided that any copyright, trademark or other notice appearing on such Materials is also retained by, displayed, copied or downloaded as part of the Materials and is not removed or obscured, and provided you do not edit, modify, alter or enhance the Materials. Please refer to our Website User Agreement for more details.

Order now!

Reprints of this article can also be ordered at

http://www.dekker.com/servlet/product/DOI/101081SS100100648